An ultra-fast scheme for sample-detection in dynamic-mode Atomic Force Microscopy

Deepak R. Sahoo, Abu Sebastian and Murti V. Salapaka

Department of Electrical and Computer Engineering, Iowa State University, Ames, IA, 50011.
{deepak, abuseb, murti}@iastate.edu.

ABSTRACT

In typical dynamic mode operation of atomic force microscopes steady state signals like amplitude and phase are used for detection and imaging of material. In these methods, high quality factor of the cantilever results in high resolution, but low bandwidth and vice versa. In this paper we present a methodology that exploits the deflection signal during the transients of the cantilever motion. The principle overcomes the limitations on the trade off between resolution and bandwidth present in existing methods and makes it independent of the quality factor. Experimental results provided corroborate the theoretical development.

Keywords: atomic force microscopy, state-space model, state observer, hypothesis testing

1 INTRODUCTION

Atomic force microscopes [1] (AFMs) utilize a cantilever to image and manipulate sample properties at the nano-scale. Cantilevers have been utilized in biological sciences to perform remarkable feats such as cutting DNA strands [2] and monitoring RNA activity [3]. On a similar note there are impressive proposals on using cantilever based nanoprobes to interrogate cell dynamics that will have significant impact on human health. At present extensive research is being carried out to develop tip-based data storage devices [4] using cantilevers as sensors and actuators for high density data storage in the range of 10^{12} bits/in^2 with data read-write rates of the order of 100 kHz. These events often have time-scales in the micro-second or nano-second regimes. Current technology does not meet the aforementioned high precision and bandwidth requirements.

The cantilever is often operated in the dynamic-mode due to its gentle nature on the sample [5]. In this mode of operation, a cantilever with high quality factor is employed for high resolution. However, due to large settling time, the steady state signals (like the demodulated amplitude or phase) of the cantilever response are slow and therefore the corresponding methods have a smaller bandwidth. Using active Q control the bandwidth can be increased [6], [7], [8]; however the trade off between bandwidth and resolution remains inherent [8]. The existing methods do not utilize the cantilever model and do not exploit the deflection signal during the transient state of the cantilever.

In this paper we present a new principle that harnesses the transient part of the cantilever dynamics. As in steady state methods, high quality factors result in high resolution; however in the method presented, the bandwidth is largely independent of the quality factor and is determined by the resonant frequency of the cantilever. As is seen later it also provides advantages with respect to resolution; particularly of events that have very small time scales.

2 SAMPLE-DETECTION

The transient signal based detection method relies on identifying the first mode model of the cantilever-dynamics and consequently construction of an observer that provides an estimate of the cantilever-dynamics. The resulting architecture facilitates the detection of tip-sample interaction force during the transient state of the cantilever as described below.

2.1 Model of the cantilever-dynamics

When the cantilever is forced sinusoidally near its first resonance frequency, its dynamic response is well described by the first mode model given by:

$$\begin{aligned} \dot{x} &= \overbrace{\begin{bmatrix} 0 & 1 \\ -\omega_0{}^2 & -\frac{\omega_0}{Q} \end{bmatrix}}^{A} x + \overbrace{\begin{bmatrix} 0 \\ 1 \end{bmatrix}}^{B} (\eta + w), \\ y &= \overbrace{\begin{bmatrix} 1 & 0 \end{bmatrix}}^{C} x + \upsilon, \end{aligned} \tag{1}$$

where the cantilever states $x = [p\ v]^T$, Q, ω_0, η, w, y and υ denote the cantilever-tip position (p) and velocity ($\upsilon = \dot{p}$), the quality factor, the first resonant frequency, the thermal-noise, external forces acting on the cantilever, the deflection signal and the photo-diode noise respectively. The cantilever model described above can be identified precisely using its thermal-noise response [9]. The cantilever can be imagined to be a system that takes in the thermal-noise η, the dither signal g and the tip-sample interaction force $\phi(x)$ as inputs (in which case $w = \phi + g$) and produces the photodiode signal y as the output.

2.2 Observer based state-estimation

The construction of the observer (see Figure 1) is based on the cantilever-model and power spectral densities of the noise. The observer dynamics is given by:

$$\begin{aligned} \dot{\hat{x}} &= A\hat{x} + Bg + L(y - \hat{y});\ \hat{x}(0) = \hat{x}_0, \\ \hat{y} &= C\hat{x}, \end{aligned} \tag{2}$$

and associated state estimation error ($\tilde{x} := x - \hat{x}$) dynamics is given by:

$$\dot{\tilde{x}} = (A - LC)\tilde{x} + B\eta - L\upsilon;\ \tilde{x}(0) = x(0) - \hat{x}(0). \tag{3}$$

The observer mimics the dynamics of the cantilever (given in Equation (1)) by utilizing the correcting term $L(y-\hat{y})$ where L is the gain of the observer and $y-\hat{y} := e$ is the error in estimating the deflection signal. The error $\tilde{x}$ between the estimated state $\hat{x}$ and the actual state x of the cantilever, when no noise terms are present ($\eta = \upsilon = 0$) is only due to the mismatch in the initial state of the observer and the cantilever (see Equation (3)). The error $\tilde{x}$ goes to zero when the real part of all the eigenvalues of the matrix $(A - LC)$ are negative. Since the pair (A, C) is *observable* for the cantilever model (i.e. $rank([A\ CA]^T) = 2$ when a second order model is assumed) the eigenvalues of the matrix $A - LC$ can be placed anywhere by appropriately choosing L [10]. Thus the error signal e due to initial condition mismatch can be reduced to zero and in principle arbitrarily fast by suitably choosing L. When there is a change in the tip-sample interaction the cantilever dynamics is effected. This introduces an error in tracking which evolves according to the cantilever-observer dynamics as given by Equation (3). Also, when the change in the tip-sample potential persists, the observer by utilizing its input y may track the altered cantilever state. It can also be shown that in the presence of noise sources η and υ the error signal e is a zero-mean stationary process. Thus the error signal e shows the signature of the change in the tip-sample behavior (buried in noise) immediately after the change is introduced. The error e may recover its zero mean nature even when the interaction change persists. This is in contrast to the steady state methods where the information is available not in the initial part but after the cantilever has come to a steady state. The Kalman observer [11] can be employed for optimal tracking in which case the error process (also known as the *innovation*) has zero mean and is white during perfect tracking.

2.3 Estimation-error characterization

The error profile due to a tip-sample interaction change can be better characterized if a model of the effect of the tip-sample interaction change on the cantilever-motion is available. We assume that the sample's influence on the cantilever tip is approximated by an impact condition where the tip-position and velocity instantaneously

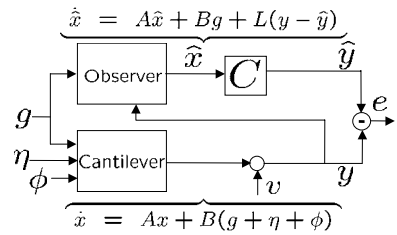

Figure 1: The observer estimates the state to be $\hat{x}$ in presence of thermal noise η and photo-diode noise υ. The actual state is x. By a choice of the observer gain L the error e in the state estimate goes to zero when the cantilever is freely oscillating. When the cantilever is subjected to the sample force ϕ, its dynamics is altered whereas the observer dynamics remains the same. This is registered as a nonzero value in the error e.

assume a new value (equivalent to resetting to a different initial condition). This is satisfied in most typical operations because in the dynamic mode, the time spent by the tip under the sample's influence is negligible compared to the time it spends outside the sample's influence [12]. The assumption is also corroborated by experimental results provided later.

The error dynamics (characterized in the Laplace domain from Equation(3)) is given by,

$$e(s) = \frac{\eta(s) + (s^2 + \frac{\omega_0}{Q}s + \omega_0^2)v(s) + (s + \frac{\omega_0}{Q})\nu_1 + \nu_2}{s^2 + (\frac{\omega_0}{Q} + l_1)s + (\omega_0^2 + l_2 + \frac{\omega_0}{Q}l_1)}, \tag{4}$$

where $[\nu_1,\ \nu_2]^T$ is the initial condition reset due to change in tip-sample interaction and $L = [l_1\ l_2]^T$ is the gain of the observer that must satisfy the stability criterion: $(\frac{\omega_0}{Q} + l_1) > 0$ and $(\omega_0^2 + \frac{\omega_0}{Q}l_1 + l_2) > 0$.

From Equation (4) it can be seen that the tracking bandwidth is characterized by,

$$B \propto \frac{\omega_0}{Q} + l_1. \tag{5}$$

Since the choice of the gain term l_1 is independent of the quality factor Q, the tracking bandwidth of the observer is effectively decoupled from Q.

From Equation(3), it can be shown that the signal to noise ratio in the error signal e due to thermal noise,

$$SNR_{th} \propto (\omega_0^2 + \frac{\omega_0 l_1}{Q} + l_2)\nu_1^2 + (\frac{\omega_0}{Q}\nu_1 + \nu_2)^2. \tag{6}$$

Thus by increasing values of l_1 and l_2, SNR_{th} and bandwidth B increase. The signal to noise ratio due to photo-diode noise is given by,

$$SNR_\upsilon = \frac{\int_0^B \frac{\omega^2\nu_1^2 + (\frac{\omega}{Q}\nu_1 + \nu_2)^2}{(\omega^2 - \omega_0^2 - l_2 - \frac{\omega_0 l_1}{Q})^2 + \omega^2(\frac{\omega_0}{Q} + l_1)^2} d\omega}{\int_0^B \frac{[(\omega^2 - \omega_0^2)^2 + (\frac{\omega\omega_0}{Q})^2]R}{(\omega^2 - \omega_0^2 - l_2 - \frac{\omega_0 l_1}{Q})^2 + \omega^2(\frac{\omega_0}{Q} + l_1)^2} d\omega}, \tag{7}$$

where the photo-diode noise υ is assumed to be white with noise power equal to R. It can be seen that SNR_υ

decreases with increasing values of l_1 and l_2. Therefore the bandwidth constraint in the detection scheme is mainly imposed by the photo-diode noise. It is evident that a desired tradeoff between signal to noise ratio and bandwidth can be obtained by an appropriate choice of l_1 and l_2 that is independent of Q. This provides considerable flexibility when compared to the existing steady state methods where Q determines the bandwidth. For typical cantilever parameters and ambient conditions, the Kalman design yields a bandwidth $B \gg \omega_0/Q$ and the innovation process carrying the signature of tip-sample interaction has a zero mean and white component. Note that the observer gain l_1 can be chosen large enough so that the cantilever state is tracked within a couple of cycles of the dither forcing. This shows that the optimal bandwidth is primarily dictated by the resonant frequency ω_0 of the cantilever.

2.4 Hypothesis-testing based detection

The sample detection problem is formulated by considering a discretized model of the cantilever (given in Equation(1)) and the impact model for the tip-sample interaction, as described by,

$$\begin{aligned} x(i+1) &= Fx(i) + Gg(i) + G_1\eta(i) + \delta_{\theta,i+1}\nu, \\ y(i) &= Hx(i) + \upsilon(i);\ i \geq 0, \end{aligned} \tag{8}$$

where $\delta_{i,j}$ denotes the dirac delta function, θ denotes the time instant when the tip-sample impact occurs and ν signifies the magnitude of the impact. It is assumed that the thermal noise and the photodiode noise are white and uncorrelated. As indicated before, given this statistics, the optimal observer is a Kalman observer [11]. With an observer having gain K (the discrete-time equivalent of L), the innovation sequence $e(i)$ is given by [13],

$$e(i) = \Upsilon(i;\theta)\ \nu + e^w(i), \tag{9}$$

where $\Upsilon(i;\theta) = [H;\ H(F-KH);\ \cdots\ H(F-KH)^{i-\theta}]$ and $e^w(i)$ is the innovation sequence when $\nu = 0$. $\Upsilon(i;\theta)$ is a dynamic profile with unknown arrival time θ. When there is no change in tip-sample interaction (i.e. $\nu = 0$) the innovation sequence has zero mean and is white [13]. When there is a change in tip-sample interaction the innovation sequence becomes nonwhite and is sum of a zero-mean and white sequence $e^w(i)$ and $\Upsilon(i;\theta)\nu$ with θ and ν unknown.

Thus the objective of detecting a change in tip-sample interaction is translated to the task of detecting the dynamic profile $\Upsilon(i;\theta)\nu$ in a zero mean white sequence. This problem can be cast in hypothesis testing framework as,

$$\begin{aligned} H_0 &: \ Y_i = e^w(i),\ i = 1,2,\ldots,n; \\ H_1 &: \ Y_i = \Upsilon(i;\theta)\ \nu + e^w(i),\ i = 1,2,\ldots,n; \end{aligned}$$

where the observed data $Y_i = e(i)$ is the innovation sequence. The dynamic profile is detected by using a likelihood ratio test [13], [14] and a decision signal is obtained.

3 EXPERIMENTAL RESULTS

The advantages of the new methodology are well demonstrated in the following experiment performed using a Digital Instruments multi-mode AFM. A cantilever with first resonance frequency $f_0 = 70.1\ kHz$ and quality factor $Q = 180$ was forced at f_0 to an amplitude of 80 nm. A 0.5 V pulse train having 1 ms time period and duty cycle of 50% was applied to the piezo-scanner holding an HOPG (Highly Oriented Pyrolytic Graphite) sample. Each pulse applied to the piezo generated a sample profile (see Figure 2) having four peaks separated by approximately 100 μs. The sample was brought close to the cantilever so that the tip would interact with the four peaks in the sample profile. Since the settling time of the cantilever is in the order of $Q/f_0 \approx 2.57\ ms$, the cantilever was interacting with the peaks in the sample profile during its transient state and it never recovered the steady state during the experiment. From the amplitude profile of the deflection signal (see Figure 2), it is not possible to detect the four peaks in the sample profile. Since the steady state data based signals are slowly varying, it can be argued that corresponding methods fail to detect the small time-scale (high bandwidth content) profiles in the sample that may arise during scanning.

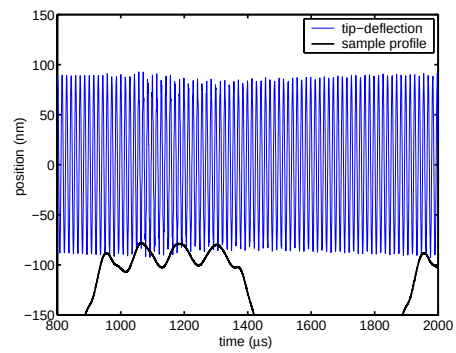

Figure 2: Cantilever-tip deflection data with respect to approximate sample position is shown. Note that from the amplitude profile of the deflection signal the four peaks in the sample profile are not discernible.

Observe that the peaks are easily discernible in the innovation sequence (see Figure 3(b)). When the cantilever is not interacting with the sample (until $\approx 950\ \mu s$) the innovation sequence has zero mean and is white. As soon as it encounters the first peak in the sample profile ($\approx 950\ \mu s$) the innovation sequence becomes nonwhite and dynamic profile is detected. Between the first and the second peaks in the sample profile, the innovation sequence recovers the zero mean and white nature until the second peak appears ($\approx 1050\ \mu s$). Overlapping dynamic profiles may appear in the innovation sequence ($\approx 1050\ \mu s$) due to multiple hits with the sample in consecutive cycles. The likelihood ratio (see Fig-

ure 3(c)) increases significantly when the dynamic profile is present in the innovation sequence. The peaks are detected within 2 cycles. The overlapping dynamic profiles are detected as a single event (second peak) as shown by the detection signal (see Figure 3(e)). Note that the cantilever has not reached steady state and is in transient during the entire experiment.

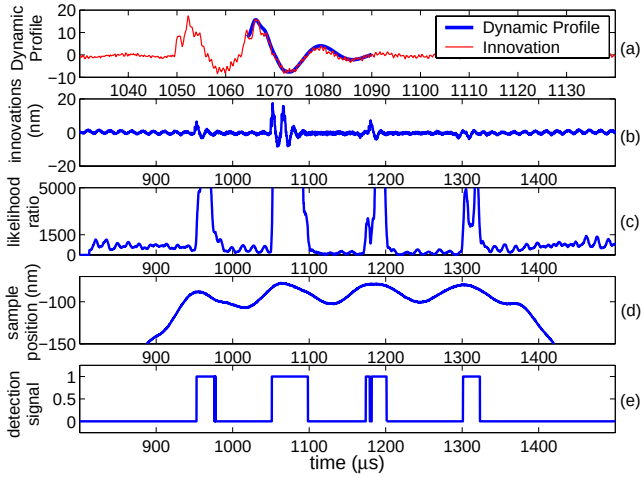

Figure 3: (a) The dynamic profile buried in innovation sequence, (b) the innovation sequence, (c) likelihood ratio, (d) sample profile and (e) the detection signal are shown when the cantilever is interacting with the sample during its transient state. The four peaks are detected by the appearance of dynamic profile in the innovation sequence and it being captured by likelihood ratio as shown by the detection signal.

The dynamic profile (see Figure 3(a)) persists for approximately 25μs ($\approx 2/f_0$ seconds) which is captured within a data window of size M=128 with a 5 MHz sampling. The dynamic profile is detected in 23.94μs ($\approx 2/f_0$ seconds) of its inception (with threshold ϵ=1681.3 corresponding to a false alarm rate of $P_F = 0.1\%$ and detection probability $P_D = 90\%$ for a minimum step size to detect ν=0.25 nm). To ensure at least one hit with cantilever the sample has to be present for more than 1 cycle ($1/f_0$ seconds) of the cantilever oscillation. A good estimate of the bandwidth is $f_0/4$ Hz=17.5 kHz. The experiment demonstrates a detection-bandwidth $\approx$ 10 kHz. This is considerably large as compared to the cantilever's natural bandwidth as determined by $f_0/Q \approx$ 390 Hz. Note that high quality factor of the cantilever does not limit the bandwidth in the proposed scheme. It is evident from the innovation sequence and the likelihood ratio that the cantilever interactions with the peaks in the sample profile are not uniform. However by feeding back the demodulated amplitude signal to the sample positioner and the cantilever this issue can be effectively addressed.

This research is supported by NSF Grant NSF ECS-0330224 to Prof. Murti V. Salapaka.

REFERENCES

[1] G. Binnig, C.F. Quate, and C. Gerber. Atomic force microscope. *Physical Review Letters*, 56(9):930–933, 1986.

[2] J. H. Hoh, R. Lal, S. A. John, J. P. Revel, et al. Atomic force microscopy and dissection of gap junctions. *Science*, 253:1405–1408, 1991.

[3] S. Kasas, N. H. Thomson, B. L. Smith, H. G. Hansma, and others. Escherichia coli rna polymerase activity observed using atomic force microscopy. *Biochemistry*, 36(3):461–468, 1997.

[4] H. J. Mamin, R. P. Ried, B. D. Terris, and D. Rugar. High-density data storage based on the atomic force microscope. *Proceedings of the IEEE*, 87(6):1014–1027, June 1999.

[5] Wisendanger. *Scanning Probe Microscopy and Spectroscopy*. Cambridge University Press, 1994.

[6] T. Sulchek, R. Hseih, J. D. Adams, G. G. Yaralioglu, S. C. Minne, C. F. Quate, J. P. Cleveland, and D. M. Adderton. High-speed tapping mode imaging with active q control for atomic force microscopy. *Applied Physics Letters*, 76:1473–1475, 2000.

[7] Tomás Rodríguez and Ricardo García. Detailed analysis of forces influencing lateral resolution for q-control and tapping mode. *Applied Physics Letters*, 79:135–137, 2001.

[8] Rainer D. Jäggi, Alfredo Franco-Obregòn, Paul Studerus, and Klaus Ensslin. Detailed analysis of forces influencing lateral resolution for q-control and tapping mode. *Applied Physics Letters*, 79:135–137, 2001.

[9] M. V. Salapaka, H. S. Bergh, J. Lai, A. Majumdar, and E. McFarland. Multimode noise analysis of cantilevers for scanning probe microscopy. *Journal of Applied Physics*, 81(6):2480–2487, 1997.

[10] Chi-Tsong Chen. *Linear System Theory and Design*. Oxford University Press, 1999.

[11] Ali H. Sayed Thomas Kailath and Babak Hassibi. *Linear Estimation*. Prentice Hall, NJ, 2000.

[12] M. V. Salapaka, D. Chen, and J. P. Cleveland. Linearity of amplitude and phase in tapping-mode atomic force microscopy. *Physical Review B.*, 61, no. 2:pp. 1106–1115, Jan 2000.

[13] Alan S. Willsky and Harold L. Jones. A Generalized Likelihood Ratio Approach to the Detection and Estimation of Jumps in Linear Systems. *IEEE Transactions on Automatic Control, pp. 108-112*, Feb. 1976.

[14] Steven M. Kay. *Fundamentals of Statistical Signal Processing, Detection Theory, vol.II*. Prentice Hall, PTR, 1993.